

AperTO - Archivio Istituzionale Open Access dell'Università di Torino

Platinum-based chemotherapy attenuates the effector response of CD8 T cells to concomitant PD-1 blockade

This is the author's manuscript

Original Citation:

Availability:

This version is available <http://hdl.handle.net/2318/1944471> since 2023-11-24T08:49:33Z

Published version:

DOI:10.1158/1078-0432.CCR-23-1316

Terms of use:

Open Access

Anyone can freely access the full text of works made available as "Open Access". Works made available under a Creative Commons license can be used according to the terms and conditions of said license. Use of all other works requires consent of the right holder (author or publisher) if not exempted from copyright protection by the applicable law.

(Article begins on next page)

Platinum-based chemotherapy attenuates the effector response of CD8 T cells to concomitant PD-1 blockade

Annapaola Mariniello^{1,2,3,4}, Tahseen H Nasti^{1,2}, Daniel Y Chang^{1,2}, Masao Hashimoto^{1,2}, Sakshi Malik^{1,2}, Daniel McManus^{1,2}, Judong Lee^{1,2}, Donald McGuire^{1,2}, Maria A Cardenas⁵, Pablo Umaña⁶, Valeria Nicolini⁶, Rustom Antia⁷, Ananya Saha⁷, Zachary S Buchwald^{4,8}, Hayden Kissick^{1,2,4,5}, Ehsan Ghorani^{1,2,9}, Silvia Novello³, Dario Sangiolo³, Giorgio V Scagliotti³, Suresh S Ramalingam^{4*} & Rafi Ahmed^{1,2,4*}

¹: Department of Microbiology and Immunology, Emory University School of Medicine, Atlanta, GA, USA

²: Emory Vaccine Center, Emory University School of Medicine, Atlanta, GA, USA

³: Department of Oncology, University of Torino, Turin, Italy

⁴: Winship Cancer Institute, Winship Cancer Institute of Emory University, Atlanta, GA, USA

⁵: Department of Urology, Emory University School of Medicine, Atlanta, GA, USA

⁶: Roche Pharma Research and Early Development, Roche Innovation Center Zurich, Schlieren, Switzerland

⁷: Department of Biology, Emory University, Atlanta, GA, USA

⁸: Department of Radiation Oncology, Emory University School of Medicine, Atlanta, GA, USA

⁹: Cancer Immunology and Immunotherapy Unit, Imperial College London, Department of Surgery and Cancer, London, UK.

*: These authors jointly supervised this work and are corresponding authors: Suresh S Ramalingam (ssramal@emory.edu) and Rafi Ahmed (email rahmed@emory.edu, mailing address: 1510 Clifton Road, Rollins Research Center, Atlanta, GA 30322)

Running title: *In vivo* effects of chemo-immunotherapy on T cell exhaustion

Conflicts of interest: Pablo Umaña and Valeria Nicolini are Roche employees, GVS received honoraria, research funding, and consultant's or advisor's fee from Roche, Pfizer, AstraZeneca, Eli Lilly, Takeda, and MSD. SN received honoraria and had roles as a consultant or advisor for AstraZeneca, Amgen, Eli Lilly, Beigene, Boehringer Ingelheim, MSD, Roche, Takeda, Pfizer, Novartis, and Sanofi. RA is an inventor on patents held by Emory University that cover the topic of PD-1-directed immunotherapy. SSR reports research support to his institution from Amgen, Merck, BMS, Astra Zeneca, Takeda and Pfizer. The remaining authors declare no competing interests.

Translational relevance

While the high anti-tumor efficacy of chemo-immunotherapy has been widely confirmed in clinical trials, we provide a proof-of-concept that current combinations could be further improved to preserve the effector response of CD8 T cells to PD-1 blockade. Using a well-established model of T cell exhaustion, we found that concomitant chemo-immunotherapy with cisplatin and pemetrexed attenuates the proliferation of antigen-specific CD8 T cells and impairs their differentiation from stem-like into effectors. As a consequence, their ability to mount an effective immune response was affected. Intriguingly, these detrimental effects were avoided using a sequential chemo-immunotherapy strategy. Overall, we provide a novel insight for reconsidering the timing of administration of chemo-immunotherapy, and prompt for further investigation of CD8 T cell functionality and long-term persistence upon combination treatments based on PD-1 blockade. Our findings have key translational relevance for lung cancer, where chemo-immunotherapy has been recently approved for disease at early-stage, with curative intent.

Abstract

Purpose: Combination of chemotherapy (CT) with programmed cell death (PD)-1 blockade is a front-line treatment for lung cancer. However, it remains unknown whether and how CT affects the response of exhausted CD8 T cells to PD-1 blockade.

Experimental design: We used the well-established mouse model of T cell exhaustion with chronic lymphocytic choriomeningitis virus (LCMV) infection to assess the effect of CT (cisplatin+pemetrexed) on T cell response to PD-1 blockade, in the absence of the impact of CT on antigen release and presentation observed in tumor models.

Results: When concomitantly administered with PD-1 blockade, CT affected the differentiation path of LCMV-specific CD8 T cells from stem-like to transitory effector cells, thereby reducing their expansion and production of interferon (IFN)- γ . After combination treatment, these restrained effector responses resulted in impaired viral control, compared to PD-1 blockade alone. The sequential combination strategy, where PD-1 blockade followed CT, proved to be superior to the concomitant combination, preserving the proliferative response of exhausted CD8 T cells to PD-1 blockade. Our findings suggest that the stem-like CD8 T cells themselves are relatively unaffected by CT partly because they are quiescent and maintained by slow self-renewal at the steady state. However, upon the proliferative burst mediated by PD-1 blockade, the accelerated differentiation and self-renewal of stem-like cells may be curbed by concomitant CT, ultimately resulting in impaired overall CD8 T cell effector functions.

Conclusions: In a translational context, we provide a proof-of-concept to consider optimizing the timing of chemo-immunotherapy strategies for improved CD8 T cell functions.

Introduction

Cancer immunotherapy with immune checkpoint blockade has revolutionized the clinical management of non-small cell lung cancer (NSCLC), which still represents the leading cause for cancer mortality worldwide (1-2). Treatment with monoclonal antibodies blocking the interaction of the coinhibitory receptor PD (programmed cell death)-1 with its main ligand PD-L1 has been shown to improve anti-tumor T cell immunity (2-5). To date, blockade of the PD-1 pathway, with anti-PD-1 or anti-PD-L1 antibodies, represents the backbone of the systemic treatment for non-oncogene addicted NSCLC (3-4). For metastatic or recurrent disease, the choice to use PD-1 blockade alone or in combination with chemotherapy (CT) and/or ipilimumab is based on PD-L1 tumor proportion score on biopsy specimen (3). In association with PD-1 blockade, the CT regimen consists of a platinum derivative (cisplatin or

carboplatin) plus pemetrexed or paclitaxel, whether the histological subtype is non-squamous or squamous (3,5).

Studies using syngeneic tumor models have already investigated the mechanisms involved in the anti-tumor activity of chemo-immunotherapy, showing that CT has immune-modulating properties and can synergize with PD-1 pathway blockade (6–9). In addition to directly reducing the tumor burden, CT has also been shown to stimulate tumor antigen release and presentation, resulting in increased activation of tumor-infiltrating lymphocytes (8-9). The magnitude of these phenomena seems to depend on the type and dose of CT, and recently the anti-folate agent pemetrexed has been shown to share these immunogenic features (10-11). On the other hand, the alkylating agent cisplatin has been reported to be a weak inducer of immunogenic cell death (9), however it was also shown that in vitro cisplatin increased CD4 T cell activation through the release of interferon (IFN)- β by monocyte-derived dendritic cells (12).

Despite the immune-modulating properties proposed above, how CT affects the proliferation and differentiation of CD8 T cells in the context of persistent antigen stimulation has yet to be addressed. For this purpose, we used the well-established murine model of T cell exhaustion with chronic lymphocytic choriomeningitis virus (LCMV) infection. This prototypical model presents the advantage to study the impact of CT on CD8 T cells that proliferate solely in response to PD-1 blockade, in the absence of the immunogenic effects of CT in terms of tumor antigen release and presentation. Using this same LCMV model, previous studies have shown how persistent antigen stimulation - as in chronic infection and cancer – upregulates PD-1 expression on T cells and leads to CD8 T cell exhaustion, a process characterized by suboptimal proliferative capacity, cytokine production, and cytotoxicity (13–15). In both mice and humans, it has now been documented that antigen-specific PD-1+ CD8 T cells are heterogeneous and composed of at least 3 subpopulations during chronic infections and cancer, recapitulating the progressive stages in the differentiation and

maintenance of exhaustion (16–21). We and others have found that the transcription factor T cell factor 1 (TCF-1) identifies a functional subset of PD-1+ CD8 T cells that is endowed with stem-like features and resides in lymphoid tissues (17,21–23). Indeed, these resource cells, also referred to as precursor of exhausted CD8 T cells, sustain the effector immune response through slow self-renewal and generation of more differentiated cells that upregulates the co-inhibitory receptor TIM-3. Within this effector population, the expression of the chemokine receptor CX3CR1 defines a circulating transitory effector subset that is highly proliferating and represents the early progeny of the stem-like CD8 T cells (18,24). Eventually, after persistent antigen exposure, virus- or tumor-specific PD-1+ CD8 T cells will further evolve into a terminally differentiated resident subset, characterized by the expression of the CD101 marker (18,23,25).

Here, our aim was to assess whether and how CT affects the CD8 T cell response to PD-1 blockade under persistent antigenic stimulation. In particular, due to the cytotoxicity of CT on highly proliferating cells, we assessed if CT affects the proliferative burst of CD8 T cells needed to generate an effective immune response upon blockade of the PD-1 pathway.

Material and methods

Experimental models

Female C57BL/6J were obtained from The Jackson Laboratory. All mouse experiments were performed with approval of the Emory University Institutional Animal Care and use Committee. For chronic LCMV, mice were infected at 6-8 weeks of age through intravenous injection with 2×10^6 pfu LCMV clone 13, according to procedures previously described (17,26). Two days before, and the same day of infection, mice were injected intraperitoneally (i.p.) with 300 ug of CD4 T cell-depleting antibody GK1.5 (Bio X Cell), as temporarily CD4 T cell depletion is required to maintain life-long systemic infection and to induce the CD8 T cell exhaustion (27). LCMV clone 13-infected CD4-temporarily depleted mice were analyzed after day 45 with blood sampling, to check for effective

infection. For acute infection, C57BL/6J mice were injected i.p. with 2×10^5 pfu LCMV Armstrong (13).

Interventions (*in vivo* experiments)

In LCMV chronically infected mice, treatment interventions started at least 45 days post-infection. CT consisted of cisplatin and pemetrexed, the first platinum-doublet approved for combination with PD-1 blockade, and still widely used for the treatment of non-squamous NSCLC (3,28). All drugs were administered i.p.. PD-1 blockade was obtained injecting 10 mg/kg of aPD-L1 (anti-mouse PD-L1 antibody; clone 10F.9G2, prepared in house) dissolved in PBS. CT was based on cisplatin and pemetrexed, purchased from Sigma-Aldrich and LC Laboratories, respectively. Cisplatin (CAS 15663-27-1) was dissolved in saline solution 0.9% and injected at the dose of 2.5 mg/kg, as in previous reports (6,29). Pemetrexed (CAS 357166-29-1) was dissolved in PBS and injected at the dose of 300 mg/kg, similar to previous reports considering treatment intensity per week (10-11,30). Cisplatin and pemetrexed were administered as separate injections, 3-6 hours following aPD-L1 injection. Conventionally, mice dosages were calculated considering 20 grams as average mice weigh.

Procedures

For the chronic LCMV infection experiments, at day 15 after treatment initiation, mice were euthanized and blood, spleen and lungs were collected and processed for lymphocyte isolation and staining for flow cytometry analyses. Spleen was also processed and analyzed for intracellular cytokine staining and plaque assay. For the acute LCMV infection experiment, mice sacrifice, spleen collection and lymphocyte isolation were performed at day 8 post-infection. Tissues from LCMV infected mice were processed as previously reported (13,31). Briefly, for isolation of lung lymphocytes, lungs were first perfused by injecting in the right ventricle with 10 mL of ice-cold phosphate-buffered saline, then

removed and trimmed with scissors. Following incubation in 0.25 mg of collagenase B (Boehringer Mannheim)/ml and 1 U/mL of DNase (Sigma) at 37°C for 60 min, the digested lungs were passed through a cell strainer and centrifuged, and the pellet was resuspended in 5 to 10 ml of 44% Percoll (Sigma). This suspension was underlaid with 67% Percoll and spun at $850 \times g$ for 20 min at room temperature, the lung lymphocyte population was harvested from the interface, and red blood cells were lysed using 0.83% ammonium chloride.

Intracellular cytokine staining experiment

2×10^6 splenocytes isolated from LCMV infected mice were incubated in RPMI with 10% FBS with 0.2 mg/mL of LCMV peptides (Gp33-41, Gp276-286) for 5 h at 37 °C in the presence of BD GolgiStop and BD GolgiPlug, according to manufacturer's protocols. After incubation, cells were stained for flow cytometry (see below).

Flow cytometry

The following antibodies were used in flow cytometry experiments: live/dead (Invitrogen, Fixable Viability Dye), CD8a (BD Biosciences, 53-6.7), CD4 (BD Biosciences, GK1.5) CD44 (BD Biosciences, IM7), TIM-3 (Biolegend, RMT3-23), PD-1 (Biolegend, 29F.1A12), CD101 (Invitrogen, Moushi101), CX3CR1 (Biolegend, SA011F11) and LCMV-specific tetramers (DbGp33-41; DbGp276-286) as surface markers, and TCF-1 (Cell Signaling, C63D9, RRID:AB_2199302), Ki-67 (BD Biosciences, B56) as intracellular markers. IFN- γ (Biolegend, XMG1.2) and TNF- α (Biolegend, MP6-XT22) were also used for intracellular cytokine staining. MHC class I tetramers were prepared in-house and used as previously described (31). Single cell suspensions were stained with antibodies and/or tetramer in PBS with 2% FBS and 2 mM EDTA for extracellular targets. For intranuclear staining, the eBioscienceTM Foxp3 Transcription Factor Staining Buffer Set (Thermo Fisher Scientific)

was used for fixation, permeabilization, and intracellular staining. Samples were acquired using a 5L Aurora-Cytek spectral flow cytometer or BD LSR II, and analyzed using FlowJo v.10 (BD Biosciences, RRID:SCR_008520).

Plaque assay

Splenic viral titers were determined by plaque assay on Vero E6 cells (RRID:CVCL_XD71) as described previously (32). Briefly, 7.5×10^5 Vero cells were plated in 35-mm wells in 6-well dishes (Costar, Cambridge, MA). The plates were incubated at 37°C and used for the assay when the cell monolayers were confluent. The medium was removed and the samples to be titrated were added to the cells (0.2 ml vol). After adsorption for 60 min at 37°C, the cells were overlaid with 3 ml of 0.5% Seakem agarose (FMC Corporation) in Medium 199 (Gibco Laboratories) supplemented with 5% heat-inactivated fetal calf serum, antibiotics, and L-glutamine. The plates were incubated for 5 d at 37°C and then overlaid with 2.0 ml of 0.5% agarose in Medium 199 containing 0.01% neutral red (Gibco Laboratories). Plaques were scored the following day.

Statistics

All experiments were done in duplicate or triplicate, and the quantified data shown in dot plots represent combined data, unless otherwise noted. Summary graphs and statistics were performed in GraphPad Prism v9.3 (RRID:SCR_002798). Statistical significance was set at a p value lower than 0.05. To test differences across the treatment groups, T-test, one-way or two-way ANOVA with multiple comparison test were used, as indicated in the figure legends.

Data Availability

The raw data generated in this study are available upon reasonable request to the corresponding author.

Results

Virus-specific CD8 T cell responses after CT, PD-1 blockade, and combination therapy of CT and PD-1 blockade during chronic LCMV infection. To directly assess the effects of chemo-immunotherapy on the effector response of CD8 T cell, we used the well-established model of T cell exhaustion with the chronic LCMV infection. Groups of chronically infected mice (≥ 45 days post-infection) were either left untreated, given CT alone, treated with aPD-L1, or given combination therapy with CT and aPD-L1 (Figure 1A). To recapitulate the treatment schedule used in cancer patients, CT, based on cisplatin and pemetrexed, and aPD-L1 were administered on the same day, every 3 days (Figure 1B). After five doses of treatment, mice were sacrificed for T cell analysis in a lymphoid (spleen) and non-lymphoid tissue (lungs), and for the quantification of splenic viral titers.

Compared to the untreated group, treatment with aPD-L1 did not change the overall number of lymphocytes in the spleen, while CT either alone or in combination with aPD-L1 induced a modest reduction of the total lymphocytes (about 1.7-fold decrease for both CT and CT + aPD-L1 groups). A similar trend was observed also for the total number of CD8 and CD4 T cells (Supplemental Figure 1A).

In the spleen, treatment with aPD-L1 alone mediated a significant expansion of PD-1⁺ and LCMV-specific (PD-1⁺) CD8 T cells, the latter of which were detected by using DbGp33 and DbGp276 tetramers (Figure 1C, D, Supplemental Figure 1B). The number of PD-1⁺ CD8 T cells more than doubled after aPD-L1, whereas such expansion was not observed after combination treatment (2.2-fold lower compared to PD-1 blockade, $p < 0.0001$). Compared to the untreated mice, PD-1⁺ CD8 T cells were significantly reduced after CT alone ($p = 0.0003$) (Figure 1D). We observed the same trend for LCMV-specific CD8 T cells, where the number of Gp33⁺ and Gp276⁺ CD8 T cells in the combination group was non-significantly higher than in the untreated mice, and significantly lower

compared to the aPD-L1 group (Figure 1D). CT alone significantly reduced the number of both Gp33+ and Gp276+ CD8 T cells (Figure 1D).

The response to PD-1 blockade in the spleen was noted also in terms of relative frequency of PD-1+ CD8 T cells, which was over 3-fold higher than the untreated group ($p < 0.0001$). The frequency of Gp33- and Gp276-specific CD8 T cells was 2.8- and 4.3-fold higher, respectively, after aPD-L1 monotherapy (Supplemental Figure 1C) compared to the untreated mice. However, the frequency of PD-1+ and LCMV-specific CD8 T cells was not significantly different between the CT and the untreated groups, or between the aPD-L1 group and the combination groups.

The analysis of PD-1+ and LCMV-specific CD8 T cells in the lung showed similar results to what was observed in the spleen across the treatment groups (Figure 1E, Supplemental Figure 1D). Overall, these results indicate that the co-administration of CT and PD-1 blockade largely abrogates the therapeutic effects of PD-1 blockade on expanding LCMV-specific CD8 T cells.

CT has detrimental effects on dividing virus-specific CD8 T cells during PD-1 blockade in chronic LCMV infection and also upon antigen encounter during acute LCMV infection. Hypothesizing that the reduced number of LCMV-specific cells in CT + aPD-L1 group compared to aPD-L1 alone group was a consequence of the detrimental effect of CT on dividing cells, we quantified proliferating PD-1+ and LCMV-specific CD8 T cells by staining them with Ki-67 (Figure 2A, B). After single-agent aPD-L1 treatment, the number of proliferating (Ki-67+) PD-1+ CD8 T cells was almost 4-fold higher compared to the untreated mice ($p = 0.03$) in the spleen (Figure 2A). In contrast, in mice receiving the CT + aPD-L1 combination there was no increase in the number of proliferating PD-1+ CD8 T cells (1.3-fold higher compared to the untreated mice, $p = 0.97$). Notably, CT affected the proliferation of PD-1+ CD8 T cells even in steady-state conditions, when administered alone. At this time point of chronic LCMV infection, the proportion of Ki-67+ PD-1+ CD8 T cells was similarly low in the untreated and CT

groups (mean of 6.7% in the untreated mice). After PD-1 blockade, the proportion of proliferating PD-1+ CD8 T cells increased to an average of 15% ($p=0.0001$ compared to untreated mice) (Figure 2A). The restrained proliferative burst of PD-1+ CD8 T cells in the CT + aPD-L1 combination group, was confirmed also by the lower relative frequency of Ki-67+ PD-1+ CD8 T cells ($p=0.04$ compared to the aPD-L1 group). Number and frequency of proliferating LCMV-specific CD8 T cells recapitulated the same trend as observed for overall PD-1+ CD8 T cells across the treatment groups (Figure 2A). In the lung, the difference in proliferating LCMV-specific cells between the aPD-L1 and the combination group was more pronounced, especially in terms of relative proportions (Figure 2B).

To further assess the cytotoxic effect of CT on proliferating CD8 T cells, we tested the same platinum-doublet in another condition characterized by an even greater proliferation - during the early effector phase of acute LCMV infection. Upon antigen encounter, newly activated CD8 T cells undergo a rapid cell division, mounting a robust effector response, with viral clearance by day 8 post-infection (13). CT was given 6 hours before inducing acute LCMV infection, and mice received two more doses at day 3 and 6 post-infection, with animal sacrifice and T cell analyses performed at day 8 (Supplemental Figure 2A). We found reduced number of both total ($p=0.0004$) and activated CD8 T cells (2.8-fold change, $p=0.002$) (Supplemental Figure 2B). On the other hand, the number of naïve CD8 T cells ($CD44^{low}$) was not reduced after CT. Consistently, the number of LCMV-specific CD8 T cells was also significantly lower in acutely infected mice receiving CT [3-fold change in the number of both Gp33 ($p=0.005$) and Gp276 ($p=0.003$) cells] (Supplemental Figure 2C). Based on these findings, CT attenuates the proliferative burst of effector CD8 T cells, both in response to PD-1 blockade in the context of persistent antigen stimulation, and in response to antigen encounter in the context of the expansion phase of acute LCMV infection.

Differential effects of CT, PD-1 blockade, and combination therapy on stem-like, transitory effector, and terminally differentiated CD8 T cell subsets during chronic LCMV infection. Once observed that CT attenuates the proliferation of CD8 T cells responding to concomitant PD-1 blockade, we assessed if any specific CD8 T cell population among LCMV-specific CD8 T cells was more vulnerable to the cytotoxicity of CT. Across treatment groups, we examined the number and frequency of the stem-like cells (PD-1+TCF-1+TIM-3-) and the more differentiated progeny of transitory effector (PD-1+CX3CR1+TIM-3+ or PD-1+CD101-TIM-3+), and terminally differentiated (PD-1+CD101+TIM-3+) LCMV-specific CD8 T cells in the spleen. Likely due to the slow self-renewal, the stem-like subset was mostly spared by the cytotoxicity of CT alone (Figure 3A). The number of stem-like cells did not change after CT compared to the untreated mice, and increased in both the aPD-L1 and the combination groups. However, the magnitude of expansion of stem-like cells tended to be greater after PD-1 blockade compared to the combination therapy, in particular for the Gp276+ CD8 T cells (1.6-fold change, $p=0.048$) (Figure 3A). Of note, the relative proportion of stem-like cells was higher in the CT group for both the Gp33+ and Gp276+ CD8 T cells compared to the groups of untreated, aPD-L1 treatment, and CT + aPD-L1 combination therapy. (Supplemental Figure 3A). These data suggest the resistance of stem-like cells to cytotoxicity, at least in their resting phase.

The transitory effector PD-1+CX3CR1+TIM-3+ CD8 T cell subset expanded after both PD-1 blockade and CT + aPD-L1 combination (Figure 3B, Supplemental Figure 3B). After aPD-L1 treatment alone, the number of transitory effector cells was 2.4-fold higher for the Gp33+ CD8 T cells ($p=0.03$) and 8-fold higher for the Gp276+ CD8 T cells ($p<0.0001$) compared to those in untreated mice. It is worth to notice that among the three subsets, the transitory effector is the only subset that increases in terms of relative frequency after treatment with aPD-L1 (from an average of 10% in the untreated mice to an average 18-20% in the aPD-L1 group). Even though the proportion of transitory effector cells did not change by adding CT to PD-1 blockade (Supplemental Figure 3B), their absolute

number was slightly lower in mice treated with CT + aPD-L1 combination compared to aPD-L1 for Gp33+ CD8 T cells (1.5-fold change, $p=0.1$) and significantly lower for Gp276+ CD8 T cells (2.2-fold change, $p=0.02$) (Figure 3B).

Terminally differentiated CD8 T cells represent the most prevalent subset at this late time-point of chronic infection, accounting for over 70% of the LCMV-specific CD8 T cells in untreated mice (18). While CT alone resulted in a decreased number of terminally differentiated LCMV-specific CD8 T cells, after PD-1 blockade these cells were significantly augmented compared to the untreated group (Figure 3C). In contrast, adding CT to PD-1 blockade abrogated the expansion of terminally differentiated CD8 T cells seen after PD-1 blockade alone [1.6-fold decrease for Gp33+ CD8 T cells ($p=0.01$) and 2-fold decrease for Gp276+ CD8 T cells ($p=0.004$)]. (Figure 3C). The relative distribution of terminally differentiated CD8 T cells was comparable across the 4 groups for the Gp33+ CD8 T cells, while for the Gp276+ CD8 T cells, the proportion was higher in the untreated and CT groups, compared to both the aPD-L1 and the combination group (Supplemental Figure 3C).

Effects of CT, PD-1 blockade, and combination treatment on proliferation of the three CD8 T cell subsets during chronic LCMV infection. We then assessed the extent of proliferation, defined by the Ki-67+ population, of stem-like (PD-1+TCF-1+TIM-3-), transitory effector (PD-1+CD101-TIM3+), and terminally differentiated (PD-1+CD101+TIM-3+) CD8 T cell subsets among LCMV-specific Gp276+ CD8 T cells across the treatment groups. Similar to what was shown by Gill et al (33), the proliferation of the stem-like subset was low at this time-point, but with numerically higher after PD-1 blockade alone (mean 4.3% in aPD-L1 vs 1.4% in untreated and 2.4% in the combination groups) (Figure 4A, B). As expected, the transitory effector subset presented the most intense proliferation, which further increased after aPD-L1 therapy (from 17% in the untreated to 41% in the aPD-L1 groups, $p<0.0001$) (Figure 4B). It should be noted that compared to single-agent aPD-L1, in the CT + aPD-L1

group, both the intensity of Ki-67 expression (Figure 4A) and the proportion of Ki-67⁺ cells within the PD-1⁺CD101⁺TIM-3⁺ subset were significantly reduced (mean value 26.7% vs 42% in the combination and the aPD-L1 group, $p=0.0002$) (Figure 4B). The frequency of Ki-67⁺ cells in the transitory effector Gp276⁺ CD8 T cells was lower also after CT compared to the untreated control (Figure 4B). In the terminally differentiated subset, Ki-67 expression slightly increased in both the groups receiving aPD-L1 (Figure 4A), and the proportion of Ki-67⁺ cells in terminally differentiated CD8 T cells was not different between mice treated with aPD-L1 and CT + aPD-L1. Overall, these findings indicate that upon concomitant PD-1 blockade, CT preferentially affects proliferating PD-1⁺CD101⁺TIM-3⁺ transitory effector cells among the three CD8 T cell subsets during chronic LCMV infection.

Impact of CT, aPD-L1 and CT + aPD-L1 combination on the ability of CD8 T cells to secrete IFN- γ .

The reduced burst of effector CD8 T cells seen after CT + aPD-L1 combination treatment, compared to aPD-L1 alone, had negative effects on the IFN- γ production of LCMV-specific CD8 T cells. Upon *ex vivo* stimulation with LCMV peptides, the number of IFN- γ producing CD8 T cells in the combination group was comparable to that in the untreated control ($p=0.3$), and lower compared to the aPD-L1 group (mean fold change 1.9, $p=0.07$) (Figure 5A, B). Consistent with the exhausted state of LCMV-specific CD8 T cells, only a small portion of CD8 T cells secreted IFN- γ in untreated mice (mean frequency 1%). In the combination therapy group, the proportion of IFN- γ producing CD8 T cells was higher than that in untreated mice, but lower compared to that in the aPD-L1 group.

The concomitant association of CT with PD-1 blockade compromises viral control. Viral titers were measured as the *in vivo* readout of the effector functions of CD8 T cells. The splenic viral load was higher in mice treated with CT + aPD-L1 combination therapy than in those treated with PD-1

blockade (2.8 mean fold change, $p=0.03$), while comparable to the untreated groups (1.7 fold lower compared to the untreated, $p=0.2$). (Figure 5C). These results demonstrate that concomitant CT + aPD-L1 has negative effects on the therapeutic efficacy of PD-1 blockade in the chronic LCMV infection.

Effects of the sequential administration of CT and PD-1 blockade on the effector response of exhausted CD8 T cells. To assess if an alternative timing of administration of CT could preserve the proliferative burst of effector CD8 T cell upon PD-1 blockade, we tested a sequential approach of CT, followed by aPD-L1. As shown in Figure 6A, chronically infected mice were treated with five doses of CT (cisplatin and pemetrexed), followed by five doses of aPD-L1 (sequential group). Both treatments were given every three days, and aPD-L1 therapy started two days after the completion of CT. This schedule was compared to the conventional concomitant combination of five doses of CT + aPD-L1 (concomitant group). During the CT phase in the sequential group, mice in the concomitant group received mock (PBS) i.p. After treatment completion, the numbers of total lymphocytes, CD8+, PD-1+ and LCMV-specific CD8 T cell in the spleen were significantly higher in the sequential group compared to the concomitant [3- and 3.8-fold change for PD-1+ ($p<0.0001$) and Gp33+ ($p=0.01$) CD8 T cells, respectively] (Supplemental Figure 4A, Figure 6B). The number of Ki67+TIM-3+PD-1+ and of Ki67+TIM-3+Gp33+ CD8 T cells was also superior after sequential combination (for Gp33 CD8 T cells, 5- fold change, $p=0.02$) (Figure 6C). The number of stem-like Gp33+ CD8 T cells was significantly lower in the concomitant group (2-fold change, $p=0.04$) (Supplemental Figure 4B-C). As for the effector compartment, both the effector transitory and the terminally differentiated LCMV-specific CD8 T cells were more abundant after sequential CT and aPD-L1 [4.4-fold change for transitory effector ($p=0.04$); 4-fold change for the terminally differentiated Gp33 ($p=0.01$) CD8 T cells] (Supplemental Figure 4B-C). In line with these findings, CD8 T cells producing IFN- γ upon *ex vivo*

stimulation with LCMV peptides significantly expanded after sequential exposure to CT and PD-1 blockade, compared to the concomitant approach (5.3-fold change, $p=0.01$) (Figure 6D).

As a results of the preserved proliferation and differentiation of LCMV-specific CD8 T cells, viral control was also improved with the sequential compared to the concomitant combination strategy, in which the viral load in the spleen was 2.8-fold higher ($p=0.0001$) (Figure 6E).

Discussion

In this study, we investigated the *in vivo* effects of the concomitant and the sequential administration of CT and PD-1 pathway blockade on T cell exhaustion. The synergistic anti-tumor activity of CT with platinum + pemetrexed and PD-1 blockade has already been proven in tumor models (10-11). Here, we explored how CT affects the T cell proliferative response to PD-1 directed therapy, and the maintenance and differentiation of CD8 T cell subsets using the chronic LCMV infection model of T cell exhaustion. Using this model, we were able to assess the cytotoxicity of CT in a more controlled environment, where CD8 T cells proliferate only in response to PD-1 directed therapy. We have found that CT has a detrimental effect on the proliferative response of CD8 T cells to concomitant PD-1 blockade, and accordingly, on the ability of CD8 T cells to produce cytotoxic cytokines, which are both necessary for a successful immune response (14). Indeed, the restrained effector functions after combination treatment eventually resulted in impaired viral control, compared to treatment with aPD-L1 alone.

Even though the differentiated effector subset was the preferential target of the cytotoxicity of CT, the stem-like population was more resilient in the 2-weeks treatment window of our experiment. So far, only memory CD8 T cells have been shown to be chemo-resistant, in both animal and human studies. It seems likely that stem-like cells survive CT due to their quiescence at the steady-state condition. However, it is possible that this is only one of the factors at play. It has been shown in

progenitor cells the existence of a cytoprotective machinery regulated at multiple levels to withstand genomic insult, thus allowing long-term survival and preventing the propagation of misrepaired DNA lesions to the downstream progeny (34–39). These mechanisms have been shown to protect epithelial stem-cells and memory CD8 T cells from genotoxins, while more differentiated CD8 T cells seem to be affected (34,35,39)(40). Based on this evidence, we can hypothesize that the contraction of the terminally differentiated subset observed in our study could be due to more than one reason. On one hand, it could be simply the result of the reduction of the upstream population of proliferating transitory effector cells; on the other hand, CT could directly induce cell death of terminally differentiated cells, potentially more vulnerable to DNA damage, compared to the less differentiated counterpart of early generated effector and stem-like cells. Future studies would be needed to confirm and thoroughly investigate the program to maintain genome integrity in exhausted CD8 T cell subsets.

The anti-tumor activity of CT mostly relies on the ability to deplete rapidly proliferating cells, a shared characteristic of chemotherapeutics, irrespective of the specific agent. Therefore, it seems plausible that the detrimental effects observed after platinum + pemetrexed on the proliferative response of CD8 T cells do not strictly depend on the type of CT. However, dedicated studies would be needed to confirm this hypothesis. In this regard, it would be clinically relevant to assess if our findings apply to the platinum-based doublet with paclitaxel, that is also widely used for treatment of patients with NSCLC, in combination with PD-1 blockade, with or without anti-cytotoxic T lymphocyte antigen-4 (CTLA4) (5).

While the high anti-tumor efficacy of chemo-immunotherapy has been widely confirmed in clinical trials, our findings provide a proof-of-concept that current combinations could be further improved in clinical practice. Our data from the timing experiment suggest that the detrimental effect of CT (alone) on the proliferation of CD8 T cell could be transient and reversible after CT discontinuation, at least in the relatively short treatment window of our experiment. The underlying

reason could be that PD-1⁺ stem-like CD8 T cells are spared when CT is administered during their quiescent phase, thus preserving their differentiation and self-renewal capacity when later exposed to PD-1 blockade, as observed in the sequential combination regimen. However, stem-like CD8 T cells appear to be more vulnerable to the cytotoxicity of CT in case of concomitant combination, in light of the accelerated self-renewal they undergo when stimulated by PD-1 blockade. As we recently described (33), this cellular mechanism confers long-term durability to the stem-like subset, counteracting the simultaneous increased differentiation into effector cells that occurs under PD-1 blockade. With this regard, it would be valuable to explore the consequences of prolonged concomitant chemo-immunotherapy on PD-1⁺ TCF-1⁺ stem-like cells. Upon the sustained differentiation into effector cells mediated by concomitant PD-1 directed therapy, an impairment in the self-renewal of stem-like cells could lead to a progressive loss of this population, compromising their long-term persistence. Investigating the long-term maintenance of the stem-like exhausted CD8 T cells after CT ± PD-1 blockade has key translational value, especially in the context of lung cancer, where the use of chemo-immunotherapy has been recently expanded to the adjuvant and neoadjuvant setting of the early stage disease, for curative intent (41–43).

Compared to the concomitant combination, a sequential strategy may spare the self-renewal and differentiation of stem-like cells boosted by PD-1 blockade. Another potential advantage of the sequential combination regimen is that the proliferative response of CD8 T cells to PD-1 blockade could be enhanced upon conditions of homeostatic proliferation, as in the case of CT-induced lymphopenia. In support of this hypothesis, in our study, the attenuation of the proliferative response in concomitant combination group was greater compared to the sequential combination than compared to PD-1 blockade alone.

Translational studies should confirm the findings we obtained in the LCMV model, with potential clinical implications on optimized timing and dosing of current and future chemo-

immunotherapy strategies. At present, NSCLC patients with evidence of clinico-radiological response after 4 cycles of platinum-based chemo-immunotherapy are eligible to maintenance immunotherapy with PD-1 blockade, that is usually combined with pemetrexed in case of non-squamous histology (3,5). In this context, our findings support the choice for a maintenance treatment based on PD-1 pathway blockade alone, and in general for a shorter CT course. Overall, the optimal duration of chemo-immunotherapy still needs to be established and it is a matter of debate in clinical practice. It should be mentioned that alternative chemo-immunotherapy combination regimens are underway or have already been approved across different tumor types (44-47).

We and others have shown that in the peripheral blood of cancer patients the expansion of PD-1+ CD8 T cells early after initiation of PD-1 blockade is predictive of clinical benefit (48-49). Our findings provide a solid rationale for the translational investigation of how the association of CT with PD-1/PD-L1 blockade can modify the magnitude or the duration of this proliferative CD8 T cell response in cancer patients. Furthermore, the recent approval of chemo-immunotherapy in the neoadjuvant setting would represent an opportunity to assess more in depth its impact on the self-renewal and differentiation of stem-like CD8 T cells, that are crucial for sustained anti-tumor immunity.

Acknowledgments: this project was supported by the National Cancer Institute of the National Institutes of Health grants P50CA217691 (to S.S.R. and R.A.) and R01AI030048 (to R.A.). The content is solely the responsibility of the authors and does not necessarily represent the official views of the National Institutes of Health.

References

1. Siegel RL, Miller KD, Fuchs HE, Jemal A. Cancer statistics, 2022. *CA A Cancer J Clinicians*. 2022 Jan;72(1):7–33.
2. Wang M, Herbst RS, Boshoff C. Toward personalized treatment approaches for non-small-cell lung cancer. *Nat Med*. 2021 Aug;27(8):1345–56.
3. Singh N, Temin S, Baker S, Blanchard E, Brahmer JR, Celano P, et al. Therapy for Stage IV

Non-Small-Cell Lung Cancer Without Driver Alterations: ASCO Living Guideline. *JCO*. 2022 Oct 1;40(28):3323–43.

4. Herbst RS, Morgensztern D, Boshoff C. The biology and management of non-small cell lung cancer. *Nature*. 2018 Jan;553(7689):446–54.
5. Hendriks LE, Kerr KM, Menis J, Mok T S, Nestle U, Passaro , et al. Non-oncogene-addicted metastatic non-small-cell lung cancer: ESMO Clinical Practice Guideline for diagnosis, treatment and follow-up. *Ann Oncol*. 2023;34(4):358–376.
6. Cubas R, Moskalenko M, Cheung J, Yang M, McNamara E, Xiong H, et al. Chemotherapy Combines Effectively with Anti-PD-L1 Treatment and Can Augment Antitumor Responses. *J Clin Oncol*. 2018 Oct 15;36(25):2273–86.
7. Apetoh L, Ghiringhelli F, Tesniere A, Obeid M, Ortiz C, Criollo A, et al. Toll-like receptor 4-dependent contribution of the immune system to anticancer chemotherapy and radiotherapy. *Nat Med*. 2007 Sep;13(9):1050–9.
8. Galluzzi L, Buqué A, Kepp O, Zitvogel L, Kroemer G. Immunological Effects of Conventional Chemotherapy and Targeted Anticancer Agents. *Cancer Cell*. 2015 Dec 14;28(6):690–714.
9. Pfirschke C, Engblom C, Rickelt S, Cortez-Retamozo V, Garris C, Pucci F, et al. Immunogenic Chemotherapy Sensitizes Tumors to Checkpoint Blockade Therapy. *Immunity*. 2016 Feb 16;44(2):343–54.
10. Lu CS, Lin CW, Chang YH, Chen HY, Chung WC, Lai WY, et al. Antimetabolite pemetrexed primes a favorable tumor microenvironment for immune checkpoint blockade therapy. *J Immunother Cancer*. 2020 Nov;8(2):e001392.
11. Schaer DA, Geeganage S, Amaladas N, Lu ZH, Rasmussen ER, Sonyi A, et al. The Folate Pathway Inhibitor Pemetrexed Pleiotropically Enhances Effects of Cancer Immunotherapy. *Clinical Cancer Research*. 2019 Dec 1;25(23):7175–88.
12. Hu J, Kinn J, Zirakzadeh AA, Sherif A, Norstedt G, Wikström AC, et al. The effects of chemotherapeutic drugs on human monocyte-derived dendritic cell differentiation and antigen presentation. *Clinical and Experimental Immunology*. 2013 Apr 18;172(3):490–9.
13. Wherry EJ, Blattman JN, Murali-Krishna K, van der Most R, Ahmed R. Viral Persistence Alters CD8 T-Cell Immunodominance and Tissue Distribution and Results in Distinct Stages of Functional Impairment. *J Virol*. 2003 Apr 15;77(8):4911–27.
14. Barber DL, Wherry EJ, Masopust D, Zhu B, Allison JP, Sharpe AH, et al. Restoring function in exhausted CD8 T cells during chronic viral infection. *Nature*. 2006 Feb;439(7077):682–7.
15. Zajac AJ, Blattman JN, Murali-Krishna K, Sourdive DJD, Suresh M, Altman JD, et al. Viral Immune Evasion Due to Persistence of Activated T Cells Without Effector Function. *Journal of Experimental Medicine*. 1998 Dec 21;188(12):2205–13.
16. Jansen CS, Prokhnevskaya N, Master VA, Sanda MG, Carlisle JW, Bilen MA, et al. An intratumoral niche maintains and differentiates stem-like CD8 T cells. *Nature*. 2019 Dec 19;576(7787):465–70.
17. Im SJ, Hashimoto M, Gerner MY, Lee J, Kissick HT, Burger MC, et al. Defining CD8+ T cells that provide the proliferative burst after PD-1 therapy. *Nature*. 2016 Sep 15;537(7620):417–21.
18. Hudson WH, Gensheimer J, Hashimoto M, Wieland A, Valanparambil RM, Li P, et al. Proliferating Transitory T Cells with an Effector-like Transcriptional Signature Emerge from PD-1+ Stem-like CD8+ T Cells during Chronic Infection. *Immunity*. 2019 Dec;51(6):1043–1058.e4.
19. Guo X, Zhang Y, Zheng L, Zheng C, Song J, Zhang Q, et al. Global characterization of T cells in non-small-cell lung cancer by single-cell sequencing. *Nat Med*. 2018 Jul;24(7):978–85.
20. Brummelman J, Mazza EMC, Alvisi G, Colombo FS, Grilli A, Mikulak J, et al. High-dimensional single cell analysis identifies stem-like cytotoxic CD8+ T cells infiltrating human tumors. *Journal of Experimental Medicine*. 2018 Oct 1;215(10):2520–35.

21. Siddiqui I, Schaeuble K, Chennupati V, Fuertes Marraco SA, Calderon-Copete S, Pais Ferreira D, et al. Intratumoral Tcf1+PD-1+CD8+ T Cells with Stem-like Properties Promote Tumor Control in Response to Vaccination and Checkpoint Blockade Immunotherapy. *Immunity*. 2019 Jan;50(1):195-211.e10.
22. Utzschneider DT, Charmoy M, Chennupati V, Pousse L, Ferreira DP, Calderon-Copete S, et al. T Cell Factor 1-Expressing Memory-like CD8+ T Cells Sustain the Immune Response to Chronic Viral Infections. *Immunity*. 2016 Aug;45(2):415–27.
23. Im SJ, Konieczny BT, Hudson WH, Masopust D, Ahmed R. PD-1+ stemlike CD8 T cells are resident in lymphoid tissues during persistent LCMV infection. *Proc Natl Acad Sci USA*. 2020 Feb 25;117(8):4292–9.
24. Hu Y, Hudson WH, Kissick HT, Medina CB, Baptista AP, Ma C, et al. TGF- β regulates the stem-like state of PD-1+ TCF-1+ virus-specific CD8 T cells during chronic infection. *Journal of Experimental Medicine*. 2022 Oct 3;219(10):e20211574.
25. Zander R, Schauder D, Xin G, Nguyen C, Wu X, Zajac A, et al. CD4+ T Cell Help Is Required for the Formation of a Cytolytic CD8+ T Cell Subset that Protects against Chronic Infection and Cancer. *Immunity*. 2019 Dec;51(6):1028-1042.e4.
26. Araki K, Morita M, Bederman AG, Konieczny BT, Kissick HT, Sonenberg N, et al. Translation is actively regulated during the differentiation of CD8+ effector T cells. *Nat Immunol*. 2017 Sep;18(9):1046–57.
27. Matloubian M, Concepcion RJ, Ahmed R. CD4+ T cells are required to sustain CD8+ cytotoxic T-cell responses during chronic viral infection. *J Virol*. 1994 Dec;68(12):8056–63.
28. Gandhi L, Rodríguez-Abreu D, Gadgeel S, Esteban E, Felip E, De Angelis F, et al. Pembrolizumab plus Chemotherapy in Metastatic Non–Small-Cell Lung Cancer. *N Engl J Med*. 2018 May 31;378(22):2078–92.
29. Chang CL, Hsu YT, Wu CC, Lai YZ, Wang C, Yang YC, et al. Dose-Dense Chemotherapy Improves Mechanisms of Antitumor Immune Response. *Cancer Research*. 2013 Jan 1;73(1):119–27.
30. Teicher BA, Chen V, Shih C, Menon K, Forler PA, Phares VG, et al. Treatment regimens including the multitargeted antifolate LY231514 in human tumor xenografts. *Clin Cancer Res*. 2000 Mar;6(3):1016–23.
31. Murali-Krishna K, Altman JD, Suresh M, Sourdive DJ, Zajac AJ, Miller JD, et al. Counting antigen-specific CD8 T cells: a reevaluation of bystander activation during viral infection. *Immunity*. 1998 Feb;8(2):177–87.
32. Ahmed R, Salmi A, Butler LD, Chiller JM, Oldstone MB. Selection of genetic variants of lymphocytic choriomeningitis virus in spleens of persistently infected mice. Role in suppression of cytotoxic T lymphocyte response and viral persistence. *Journal of Experimental Medicine*. 1984 Aug 1;160(2):521–40.
33. Gill AL, Wang PH, Lee J, Hudson WH, Ando S, Araki K, et al. PD-1 blockade increases the self-renewal of stem-like CD8 T cells to compensate for their accelerated differentiation into effectors. *Sci Immunol*. 2023;8(86):eadg0539.
34. Gottesman MM, Fojo T, Bates SE. Multidrug resistance in cancer: role of ATP-dependent transporters. *Nat Rev Cancer*. 2002 Jan 1;2(1):48–58.
35. Turtle CJ, Swanson HM, Fujii N, Estey EH, Riddell SR. A Distinct Subset of Self-Renewing Human Memory CD8+ T Cells Survives Cytotoxic Chemotherapy. *Immunity*. 2009 Nov;31(5):834–44.
36. Mohrin M, Bourke E, Alexander D, Warr MR, Barry-Holson K, Le Beau MM, et al. Hematopoietic Stem Cell Quiescence Promotes Error-Prone DNA Repair and Mutagenesis. *Cell Stem Cell*. 2010 Aug;7(2):174–85.
37. Sheng X, Lin Z, Lv C, Shao C, Bi X, Deng M, et al. Cycling Stem Cells Are Radioresistant and Regenerate the Intestine. *Cell Reports*. 2020 Jul;32(4):107952.

38. Johnnidis JB, Muroyama Y, Ngiow SF, Chen Z, Manne S, Cai Z, et al. Inhibitory signaling sustains a distinct early memory CD8⁺ T cell precursor that is resistant to DNA damage. *Sci Immunol*. 2021 Jan 8;6(55):eabe3702.
39. Seita J, Rossi DJ, Weissman IL. Differential DNA Damage Response in Stem and Progenitor Cells. *Cell Stem Cell*. 2010 Aug;7(2):145–7.
40. Yan Y, Cao S, Liu X, Harrington SM, Bindeman WE, Adjei AA, et al. CX3CR1 identifies PD-1 therapy–responsive CD8⁺ T cells that withstand chemotherapy during cancer chemoimmunotherapy. *JCI Insight*. 2018 Apr 19;3(8):e97828.
41. Leal TA, Ramalingam SS. Neoadjuvant therapy gains FDA approval in non-small cell lung cancer. *Cell Reports Medicine*. 2022 Jul;3(7):100691.
42. Forde PM, Spicer J, Lu S, Provencio M, Mitsudomi T, Awad MM, et al. Neoadjuvant Nivolumab plus Chemotherapy in Resectable Lung Cancer. *N Engl J Med*. 2022 May 26;386(21):1973–85.
43. Felip E, Altorki N, Zhou C, Csőszi T, Vynnychenko I, Goloborodko O, et al. Adjuvant atezolizumab after adjuvant chemotherapy in resected stage IB–IIIA non-small-cell lung cancer (IMpower010): a randomised, multicentre, open-label, phase 3 trial. *The Lancet*. 2021 Oct;398(10308):1344–57.
44. Rocco D, Della Gravara L, Franzese N, Maione P, Gridelli C. Chemotherapy plus single/double immunotherapy in the treatment of non-oncogene addicted advanced non-small cell lung cancer: where do we stand and where are we going? *Expert Review of Anticancer Therapy*. 2022 Feb 1;22(2):183–9.
45. Paz-Ares L, Ciuleanu TE, Cobo M, Schenker M, Zurawski B, Menezes J, et al. First-line nivolumab plus ipilimumab combined with two cycles of chemotherapy in patients with non-small-cell lung cancer (CheckMate 9LA): an international, randomised, open-label, phase 3 trial. *The Lancet Oncology*. 2021 Feb;22(2):198–211.
46. Xing W, Zhao L, Zheng Y, Liu B, Liu X, Li T, et al. The Sequence of Chemotherapy and Toripalimab Might Influence the Efficacy of Neoadjuvant Chemoimmunotherapy in Locally Advanced Esophageal Squamous Cell Cancer—A Phase II Study. *Front Immunol*. 2021 Dec 6;12:772450.
47. Rutten VC, Salhi Y, Robbrecht GJ, De Wit R, Van Leenders GJLH, Zuiverloon TCM, et al. The CHASIT study: sequential chemo-immunotherapy in patients with locally advanced urothelial cancer – a non-randomized phase II clinical trial. *BMC Cancer*. 2023 Jun 13;23(1):539.
48. Kamphorst AO, Pillai RN, Yang S, Nasti TH, Akondy RS, Wieland A, et al. Proliferation of PD-1⁺ CD8 T cells in peripheral blood after PD-1–targeted therapy in lung cancer patients. *Proc Natl Acad Sci USA*. 2017 May 9;114(19):4993–8.
49. Huang AC, Postow MA, Orlovski RJ, Mick R, Bengsch B, Manne S, et al. T-cell invigoration to tumour burden ratio associated with anti-PD-1 response. *Nature*. 2017 May;545(7652):60–5.

Figure legends

Figure 1. Chemotherapy has detrimental effect on the response of LCMV-specific CD8 T cells to PD-1 blockade. (A) Experimental design. (B) Treatment regimen and schedule. (C) Representative FACS plots showing frequency of PD-1⁺, Gp33⁺ and Gp276⁺ CD8 T cells in the spleen across treatment groups. The lower box shows the % of PD-1⁺ CD8 T cells, and the upper box shows the % of tetramer⁺ CD8 T cells. Number of PD-1⁺ and LCMV-specific CD8 T cells in the spleen (D) and lung (E). Data are pooled from 2-3 independent experiments of 3-5 mice per group. For statistical

analysis the one-way ANOVA test was used; total numbers were Log_{10} transformed. Bars represent mean and SEM. * $p < 0.05$; ** $p < 0.01$; *** $p < 0.001$; **** $p < 0.0001$.

Figure 2. Chemotherapy attenuates the proliferative burst of virus-specific CD8 T cells responding to concomitant PD-1 blockade during chronic LCMV infection. (A-B) Number (first row) and relative % (second row) of proliferating (Ki-67+) PD-1+ CD8 T cells, Gp33+, and of Gp276 + CD8 T cells in the spleen (A) and in the lung (B). Data are pooled from 2-3 experiments of 4-5 mice per group. For statistical analysis the one-way ANOVA test was used; total numbers were Log_{10} transformed. Bars represent mean and SEM. * $p < 0.05$; ** $p < 0.01$; *** $p < 0.001$; **** $p < 0.0001$.

Figure 3. Stem-like CD8 T cells are resistant but transitory effector and terminally differentiated CD8 T cells are vulnerable to the cytotoxicity of chemotherapy during chronic LCMV infection. (A-C) Representative FACS plot (gated on Gp276+ CD8 T cells) with number of stem-like (PD-1+TCF-1+TIM-3-) (A), of transitory effector (PD-1+CX3CR1+TIM-3+) (B), and of terminally differentiated (PD-1+CD101+TIM-3+) (C) Gp276+ and Gp33+ CD8 T cells in the spleen across treatment groups. Data are pooled from 2-3 experiments of 4-5 mice per group. For statistical analysis the one-way ANOVA test was used; total numbers were Log_{10} transformed. Bars represents mean and SEM. * $p < 0.05$; ** $p < 0.01$; *** $p < 0.001$; **** $p < 0.0001$.

Figure 4. Chemotherapy preferentially affects the proliferation of the transitory effector CD8 T cell subset among virus-specific CD8 T cells during chronic LCMV infection. (A) Representative FACS histograms showing the expression of Ki-67 on stem-like (PD-1+TCF-1+TIM-3-), transitory effector (PD-1+CD101-TIM-3+), and terminally differentiated (PD-1+CD101+TIM-3+) subsets in Gp276+ CD8 T cells. (B) Frequency of proliferating (Ki-67+) cells within stem-like, CD101-TIM-3+, and CD101+TIM-3+ Gp276+ CD8 T cells. Data are representative of 2 experiments of 3-5 mice per group (A) or pooled from 2 independent experiments of 3-5 mice per groups (B). For statistical analysis the 2-way ANOVA test was used. Bars represent mean and SEM. * $p < 0.05$; ** $p < 0.01$; *** $p < 0.001$; **** $p < 0.0001$.

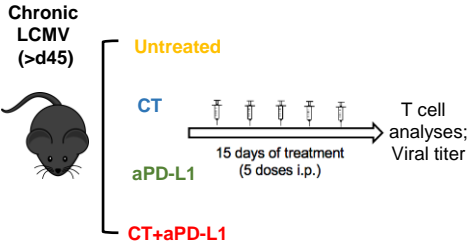
Figure 5. The combination of chemotherapy with PD-1 blockade compromises viral control. (A) Representative FACS plot of IFN- γ producing CD8 T cells after ex vivo stimulation with LCMV

peptides across treatment groups. (B) Frequency and number of IFN- γ producing CD8 T cells. Data are pooled from 3 independent experiments of 3-5 mice per group. C) Viral titers in the spleen (Log_{10} number of plaque forming units/g of tissue). Data are representative of 1 out of 3 independent experiments of 3-5 mice per group. For statistical analysis the one-way ANOVA test was used, total numbers were Log_{10} transformed. Bars represent mean and SEM. * $p < 0.05$; ** $p < 0.01$; *** $p < 0.001$; **** $p < 0.0001$.

Figure 6. The sequential administration of chemotherapy and PD-1 blockade preserves the effector response of virus-specific CD8 T cells during chronic LCMV infection. A) Experimental design. (B) Number of PD-1+ and Gp33+ CD8 T cells in the spleen in the two treatment groups. (C) Representative FACS plots showing the frequency of proliferating (TIM-3+Ki67+) PD-1+ and Gp33+ CD8 T cells in the spleen across the treatment groups, with quantified number on the right. (D) Number of IFN- γ producing CD8 T cells in the spleen. (E) Viral titers in the spleen (plaque forming units/g of tissue) across the two groups of treated mice. Data are pooled from 2 independent experiments of 4-6 mice per group. For statistical analysis the T-test was used; total numbers were Log_{10} transformed. Bars represent mean and SEM. * $p < 0.05$; ** $p < 0.01$; *** $p < 0.001$; **** $p < 0.0001$.

Figure 1

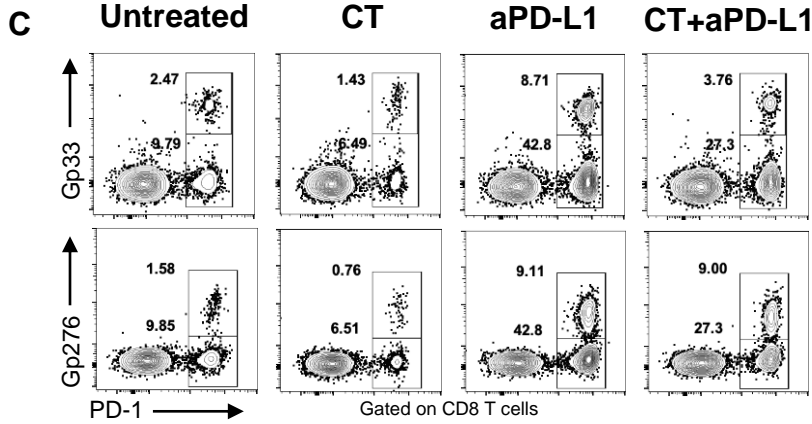
A



B

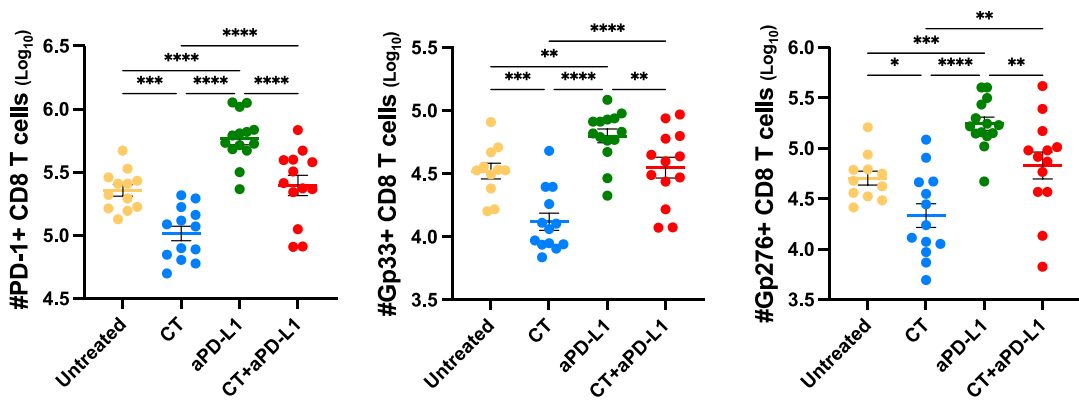
Agent	Dose*	Regimen	Route
Cisplatin	2.5 mg/kg	every 3 days for 2 weeks	IP
Pemetrexed	300 mg/kg	every 3 days for 2 weeks	IP
Anti-PD-L1	10 mg/kg	every 3 days for 2 weeks	IP

* Considering 20 g per mouse



D

Spleen



E

Lung

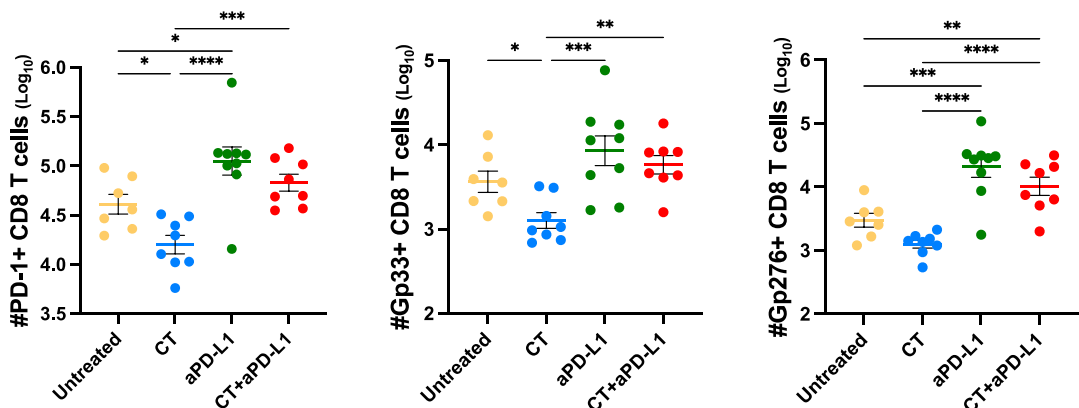
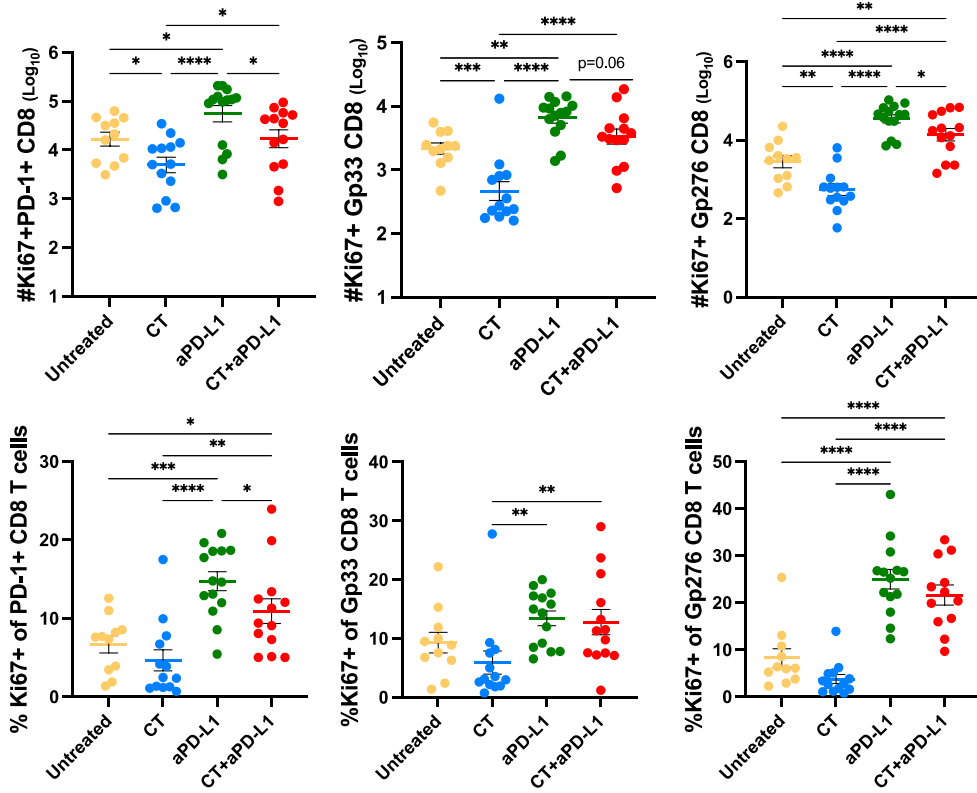


Figure 2

A

Proliferating PD-1+ and LCMV-specific CD8 T cells (spleen)



B

Proliferating PD-1+ and LCMV-specific CD8 T cells (lung)

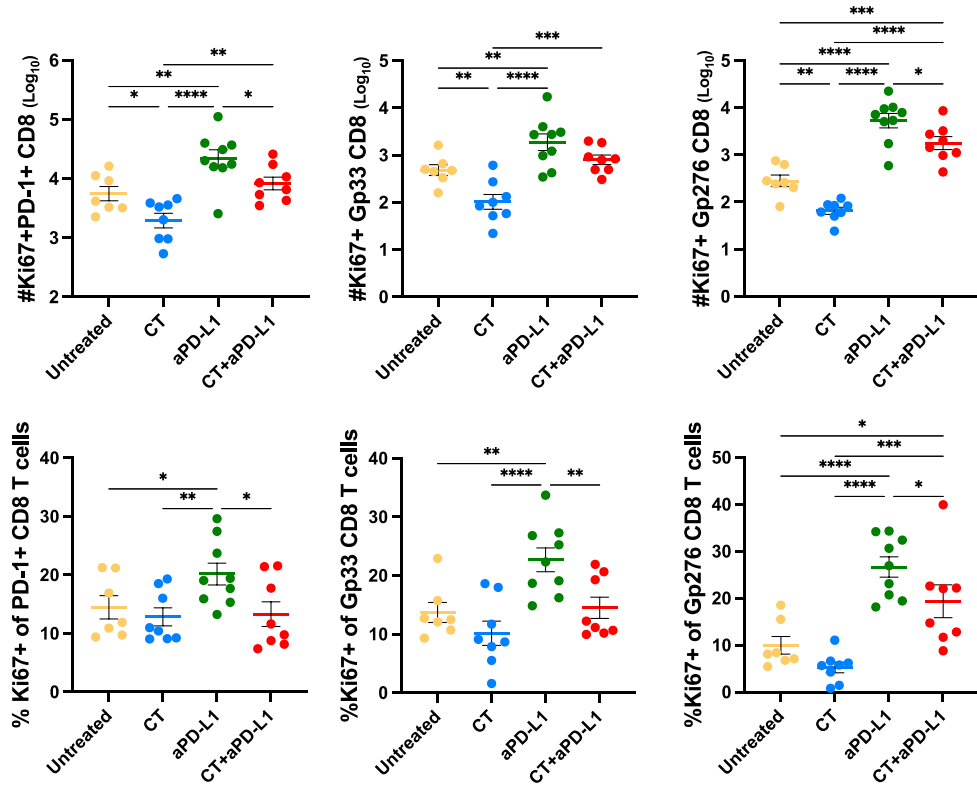


Figure 3

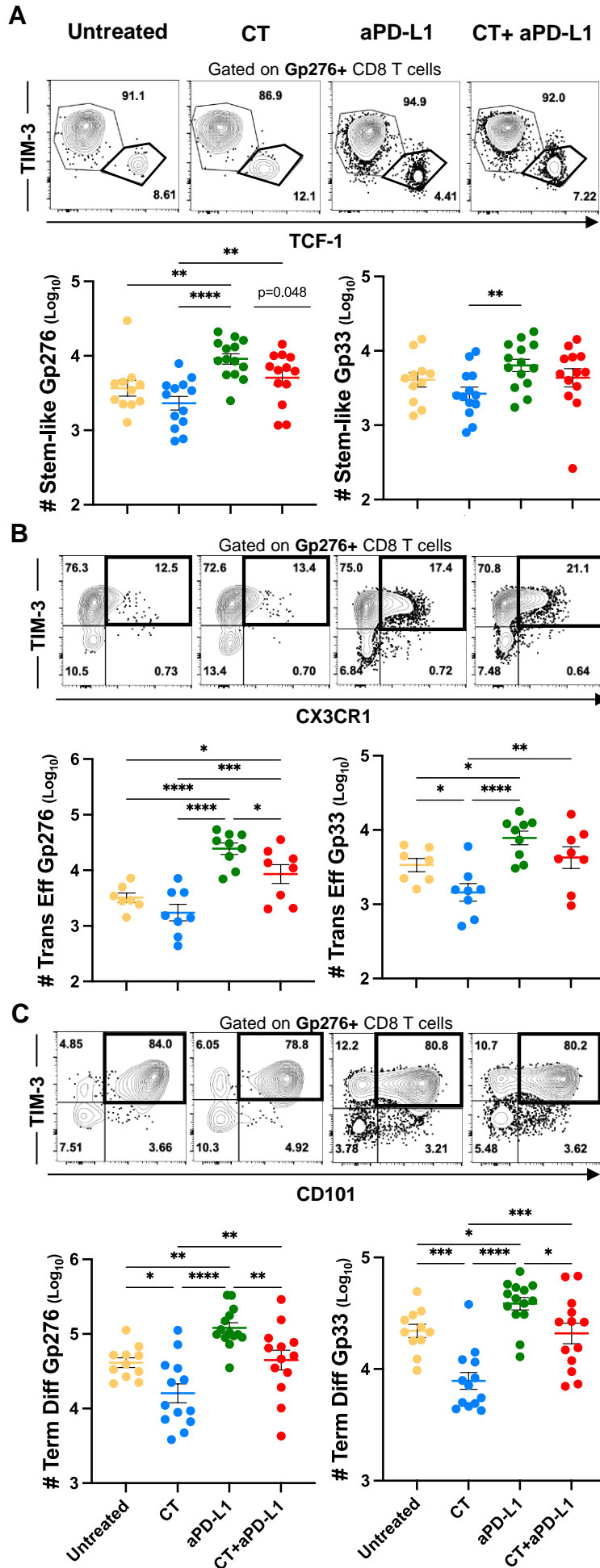


Figure 4

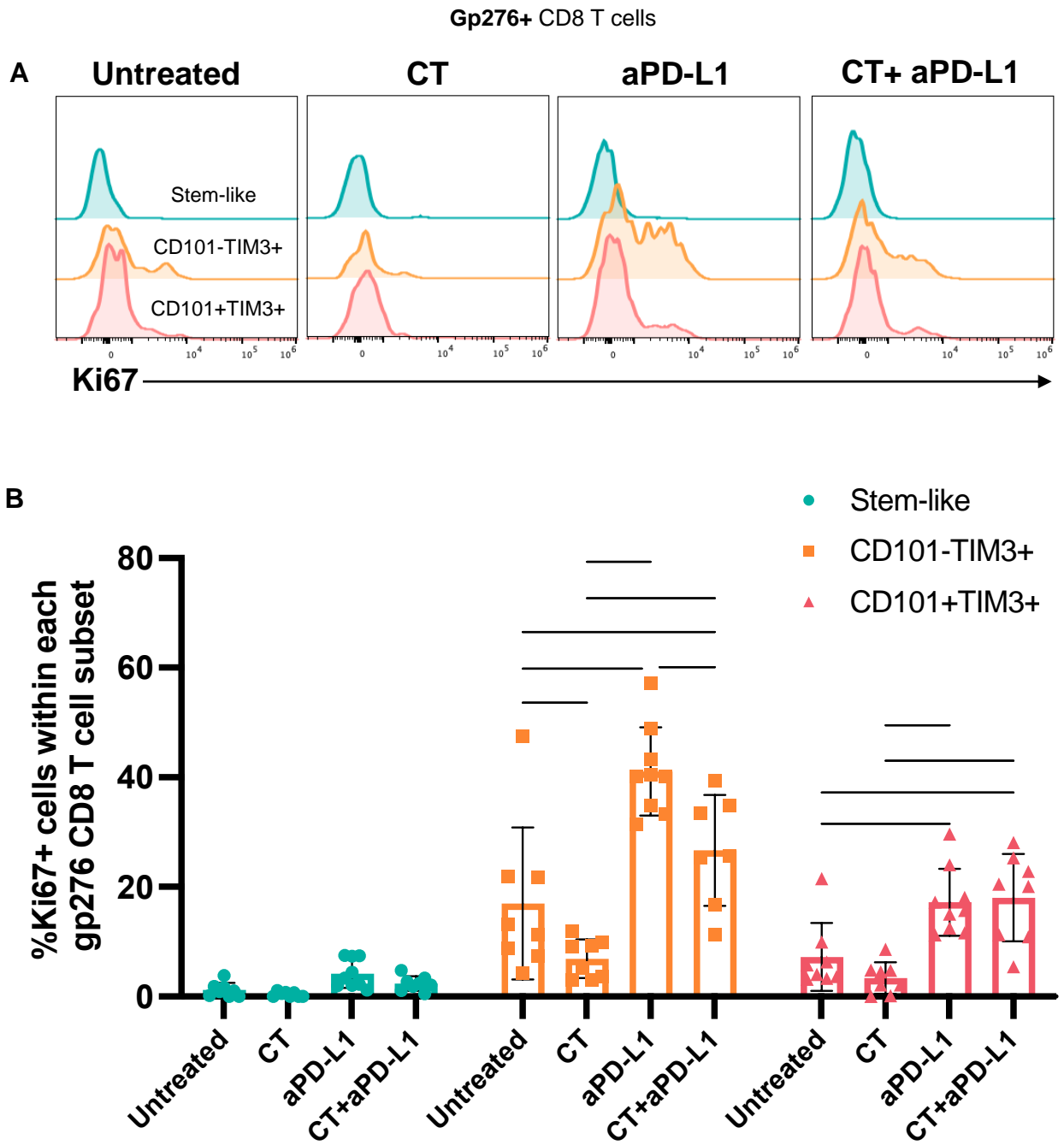


Figure 5

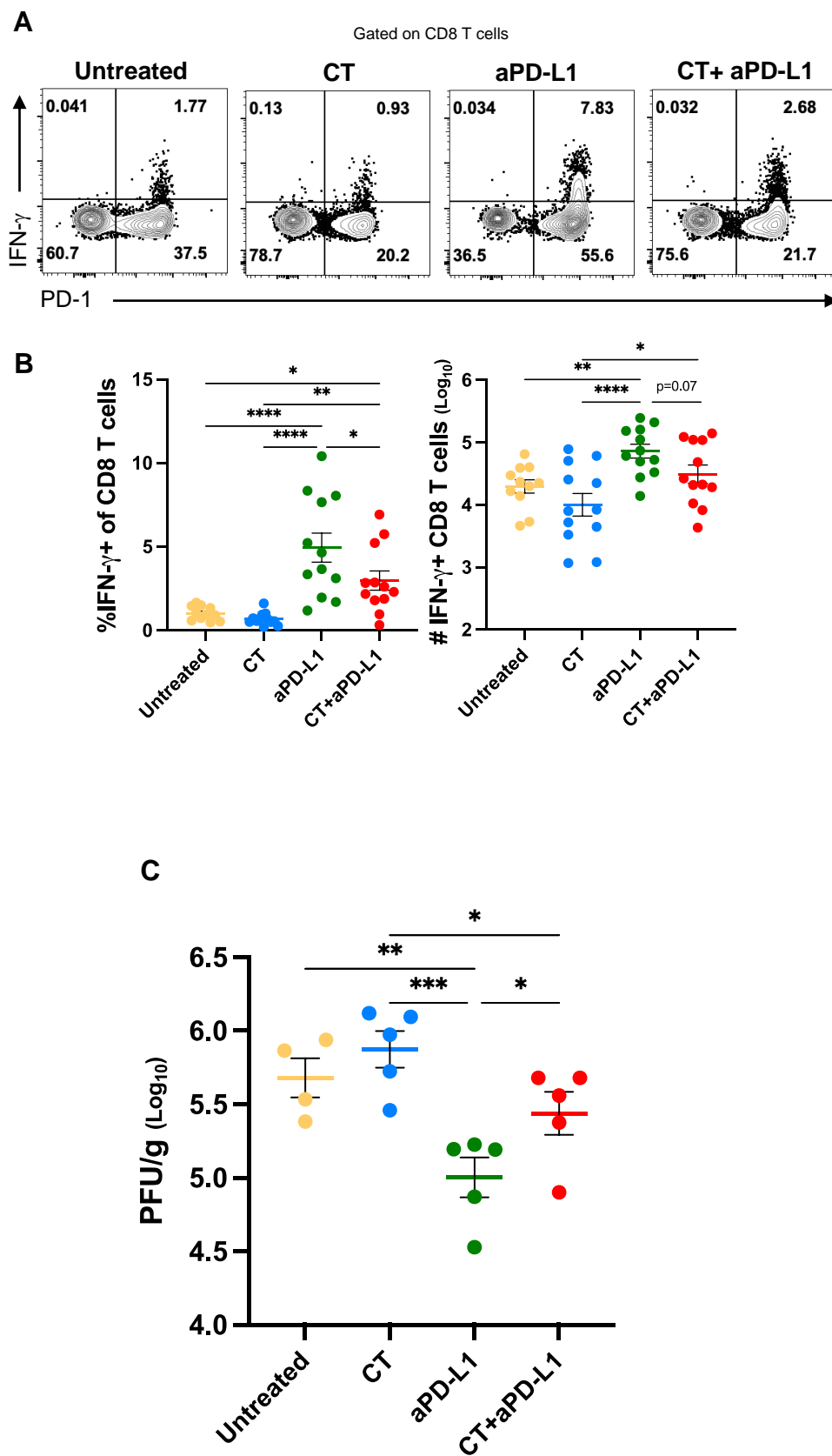


Figure 6

